action. The diabatic representation used allows us to include such additional degrees of freedom in a straightforward manner, namely by adding the corresponding wave functions to the initial and final states of the process and including the dependence of the coupling operator on the new coordinate. In the adiabatic approximation, on the other hand, the additional degree of freedom has usually been introduced as an oscillation of the barrier. In this approach, the two degrees of freedom are not treated equivalently, and off-diagonal matrix elements of the low-frequency oscillator are neglected.

In principle, our treatment can be further improved by including additional degrees of freedom. While it is not difficult to formulate such a generalized model, the parameters required for application to real systems are not normally available. The density-of-states function $\rho(\epsilon)$ implicitly includes additional motions, which are required to make the transfer irreversible, but these are treated in a much more approximate manner. The replacement of the corresponding vibrational structure by an unresolved broad band, namely a Gaussian in our case, will become strictly valid only in the limit of a very high level density which in practice will usually mean a large exothermicity. It is certainly not justified in the case of zero exothermicity where the transfer would be reversible. However, in practice one can usually measure only those reactions that are unidirectional and develop exponentially in time: in these cases the final state can always be represented by a continuum.

If the exothermicity is small, the density of states is roughly the same in the initial and final state. To simulate the effect of broadening of the initial state, we can add, as a third degree of freedom, a very low-frequency oscillation which affects the transfer indirectly by being coupled to the other oscillators. As a result, a single term in the two-mode model will now be represented by a sum of terms in the three-mode model, but the total contribution to the transfer will not change. The splitting will, however, affect the temperature dependence, namely at temperatures low enough to cause uneven population of the new manifold. At temperatures where adjacent levels of the new oscillator have virtually the same population, the effect of the splitting will be insignificant. At low temperatures, however, the transfer will not become temperature independent, as in the two-mode model, but retain a weak temperature dependence as long as $k(T)$ is above the level spacing of the third mode. It follows that for small exothermicities and low temperatures, we may expect significant deviations from the predictions of the model.

To gain further insight into its properties, we shall apply this model in the following paper in this issue[11] to a number of hydrogen-transfer reactions reported in the literature. In a future paper, we shall consider an extension of the model to three or more degrees of freedom. We believe, however, that in its present, simple form, the model can give a physically meaningful analysis of most hydrogen-transfer reactions in condensed systems.

Golden Rule Treatment of Hydrogen-Transfer Reactions. 2. Applications†

Willem Siebrand,* Timothy A. Wildman,‡ and Marek Z. Zgierski

Contribution from the Division of Chemistry, National Research Council of Canada, Ottawa, Canada K1A 0R6. *Received November 9, 1983*

Abstract: The model developed in part 1 (preceding paper) is applied to data ascribed in the literature to hydrogen (deuterium) tunneling. The transfer reactions considered are of the type AH(D) + B → A + H(D)B, where A and B are carbon, nitrogen, or oxygen atoms attached to other atoms or groups. The model consists of crossing AH- and BH-stretching potentials together with an AB vibrational potential; the two vibrational motions are assumed adiabatically separable. Spectroscopic information is used to describe the AH and BH potentials. If A, H, and B are not collinear, the AH and BH frequencies are represented by linear combinations of bending and stretching frequencies according to fixed rules. The transfer distance, defined as the shortest distance between the two equilibrium positions of the hydrogen atom, is determined from molecular models. The AB potential and the coupling between the AH and BH potentials are treated as adjustable parameters, subject to restrictions determined by the nature of the transfer. Harmonic as well as anharmonic AB potentials are considered in the following applications to hydrogen and deuterium transfer reactions: (i) isomerization of 2,4,6-tri-*tert*-butylphenyl to 3,5-di-*tert*-butylneophyl; (ii) tautomerization to 2-methylacetophenone from the cis enol; (iii) 1,4-sigmatropic hydrogen transfer in a hexahydrocarbazole; (iv) hydrogen abstraction by free radicals in crystalline dimethylglyoxime; and (v) hydrogen transfer from dihydrophenanthrene to oxygen. Also briefly considered are (vi) hydrogen abstraction by methyl radicals in organic solids and (vii) tautomerization of *meso*-tetraphenylporphine. In general the rate constants for these reactions show a non-Arrhenius temperature dependence and a large deuterium effect. In most cases, the model can account successfully for these observations in terms of physically reasonable parameter values. Discrepancies are noted and traced back to limitations of the model in its present form, indicating directions for further development. The analysis leads to new insight into the mechanism of several of the reactions. It is concluded that the present treatment is physically more realistic and quantitatively more accurate than conventional tunneling treatments.

Part 1 of this series[1] describes a theoretical model developed to calculate rate constants for reactions in which hydrogen transfer occurs by tunneling, i.e., by a nonclassical mechanism. The model is not based on the conventional tunneling formalism, however, but on the golden rule of time-dependent perturbation theory. Correspondingly, the input parameters are not the height and width of the barrier through which the hydrogen atom tunnels but are vibrational parameters describing the initial and final states of the transfer process together with a coupling. The purpose of this reformulation is to make maximum use of the available spectroscopic information so as to reduce the arbitrariness of the description. An immediate consequence of this tightening of the

† Issued as NRCC No. 23387.
‡ Research Associate.

(1) Siebrand, W.; Wildman, T. A.; Zgierski, M. Z. *J. Am. Chem. Soc.*, preceding paper in this issue.

0002-7863/84/1506-4089$01.50/0 Published 1984 by the American Chemical Society

rules has been the necessity of considering not only the motion of the hydrogen atom itself but also the thermal motion of the atoms carrying the hydrogen.

In the present paper we use this approach to treat a number of hydrogen-transfer reactions that exhibit nonclassical behavior, such as a strong deviation of the temperature dependence from the Arrhenius rate law and a deuterium isotope effect far outside the normal range of kinetic isotope effects. Our first aim is simply to show that the model can account for the observed rate constants and their temperature and isotope dependence with reasonable parameter values. In addition, we investigate the extent to which this analysis can provide information on reaction mechanisms. The reactions to be analyzed are chosen on the basis of the completeness of the available information; however, we do restrict ourselves to reactions in which the relative motion of the atoms between which the hydrogen is transferred is oscillatory rather than diffusive. The number of reactions for which rate constants are available over a wide range of temperatures for both hydrogen and deuterium transfer is small. All of these reactions are considered here; any omission is unintentional.

To show how the method works, we use simple, practical forms of the model which do not require a great deal of preparation. The formulas involve two sets of input parameters, namely, a set based on spectroscopic and structural data not subject to adjustment and a set of adjustable parameters. It is essential, of course, to keep the latter set as small as possible. It is also necessary that the values adopted for these parameters are physically reasonable; ideally they should provide additional useful information about the reaction mechanism. Unfortunately, the two requirements of minimizing the number of adjustable parameters and maximizing the amount of new information to be extracted from them tend to be contradictory. In view of the diminishing returns, a practical limit must be set on the degree of complexity to be permitted.

Two levels of complexity are compared here. In the simplest version of the model the two periodic motions, namely that of the hydrogen atom and the relative motion of the atoms carrying the hydrogen, are taken to be harmonic. In the second version the latter is allowed to be anharmonic. This introduces an additional adjustable parameter but only for the oscillator which is directly responsible for the observed temperature dependence. It is therefore justified only if the observed rate constants cover a wide range of temperatures.

1. Basic Formulas

The model to be used is that considered in section 4 of part 1. A hydrogen is transferred according to the reaction AH + B → A + HB, where A and B are molecules in a solid or groups within a molecule or complex. The AH and BH vibrations are assumed to be harmonic if A and B are non-interacting; their interaction J_{AB} causes the transfer. The relative motion of the atoms of A and B carrying the hydrogen before and after the transfer, respectively, are represented by a harmonic or an anharmonic potential of much lower frequency than the AH and BH potentials. The two vibrations are taken to be adiabatically separable, so that the total vibrational energy $\epsilon_{v,V}$ is the sum of the energies of the two oscillators, $\epsilon_v + \epsilon_V$, where

$$\epsilon_v = (v + \tfrac{1}{2})\hbar\omega$$

$$\epsilon_V = (V + \tfrac{1}{2})\hbar\Omega + \text{anharmonic terms} \quad (1)$$

For a given combination of initial quantum numbers v, V and final quantum numbers w, W, the rate constant is given by

$$k_{BA,wWvV} = (2\pi/\hbar)\rho(\epsilon_{w,W} - \epsilon_{v,V})|\langle\Lambda_W|J_{AB}S_{wv}|\Lambda_V\rangle|^2 \quad (2)$$

according to eq 21 of part 1. The density of (energy-conserving) final states is represented by a Gaussian line shape function

$$\rho(\epsilon_{w,W} - \epsilon_{v,V}) = \pi^{-1/2}\Gamma^{-1}\exp[-(\epsilon_{w,W} - \epsilon_{v,V})^2/\Gamma^2] \quad (3)$$

with a half-width Γ taken equal to $\hbar\Omega/2$. This makes ρ a smooth function of the exothermicity of the reaction. The overlap integral S_{wv} is defined as

$$S_{wv} = \langle\chi_w(r - \bar{r}_B)|\chi_v(r - \bar{r}_A)\rangle = \langle\chi_w(r + R/2 - \xi)|\chi_v(r - R/2 + \xi)\rangle \quad (4)$$

where 2ξ is the sum of the AH and BH equilibrium bond lengths. If χ is a harmonic oscillator function, this integral can be evaluated analytically by standard methods.[2] For data obtained at low temperatures ($k_BT << \hbar\omega$), we can set $v = 0$; in the special case where the AH and BH oscillator have the same frequency, eq 4 then reduces to

$$S_{w0} = \gamma^{w/2}\exp(-\gamma/2)/(w!)^{1/2} \quad (5)$$

where

$$\gamma = (\mu\omega/2\hbar)(R - 2\xi)^2 \quad (6)$$

μ being the reduced mass, assumed to be the same for these two oscillators. In general we calculate μ for an XH bond with the standard formula $\mu = m_Xm_H/(m_X + m_H)$, where m represents an atomic mass, and allow different frequencies and effective masses for the AH and BH oscillators.

In addition to S_{wv}, we also take J_{AB} to be a function of R, namely proportional to the electronic overlap between the orbitals which form the AH and BH bonds. For Slater-type orbitals, it is approximated by

$$J_{AB} = \bar{J}\exp[-\zeta(R - \bar{R})/a_0] \quad (7)$$

where $\bar{J} = J_{AB}(\bar{R})$, the value at the equilibrium separation of A and B, a_0 is the Bohr radius, and ζ is an orbital exponent[3] which depends on the nature of A and B.

To carry out the integration over R, we need to choose wave functions $\Lambda(R)$. We consider both harmonic and anharmonic wave functions, but we postpone the discussion of the latter until the next section. In general, these integrals are performed numerically for all combinations of vibrational quantum numbers. The resulting rate constants $k_{BA,wWvV}$ are summed over w and W to determine the rate constant for a given initial state v, V. To obtain the temperature-dependent rate constant $k(T)$, we calculate the thermal average over v, V:

$$k(T) = \sum_V\sum_v\Big(\sum_W\sum_w k_{BA,wWvV}\Big)\exp(-\beta\epsilon_{v,V})\Big/\sum_V\sum_v\exp(-\beta\epsilon_{v,V}) \quad (8)$$

where $\beta = (k_BT)^{-1}$.

2. Anharmonicity of the Low-Frequency Mode

In the systems to be discussed, thermal excitation of the high-frequency oscillator is usually not significant in the temperature range studied experimentally, so the observed temperature dependence is due to thermal excitation of the low-frequency mode. We therefore expect that the anharmonicity of this mode affects the temperature dependence. In our simple model, this mode represents a number of normal modes that participate in the transfer: it is thus not possible to determine the anharmonicity a priori. An illustration of the effect of anharmonicity on the hypothetical example from part 1, i.e., the reaction $CH_4 + CH_3\cdot \rightarrow CH_3\cdot + CH_4$ with CHC collinear and arbitrary parameter values, is presented in Figure 1. The dashed curves correspond to the harmonic version of the model. It may be seen in eq 2 and 8 that anharmonicity affects the rate constants in two ways: by influencing the vibrational integral for a given initial and final state and by increasing (positive anharmonicity) or decreasing (negative anharmonicity) the energy level spacing with increasing vibrational quantum numbers.

Of the anharmonic potentials investigated, the Morse potential turns out to be unsatisfactory for the low-frequency mode. Because the Morse potential rises more quickly than a harmonic potential as $R \rightarrow 0$, the individual rate constants $k_{BA,wWvV}$ are smaller for the Morse potential and the absolute rates are lower. Moreover, the $k_{BA,wWvV}$ increase more slowly with vibrational quantum number if the Morse potential is used; the slope $d(\ln k)/dT$ of the dotted curve in Figure 1 is lower than that for the harmonic potential, even though the contributions from higher quantum levels of the Morse potential are favored by the Boltzmann factor

(2) Manneback, C. *Physica (Utrecht)* **1951**, *17*, 1001.
(3) Slater, J. C. *Phys. Rev.* **1930**, *36*, 57.

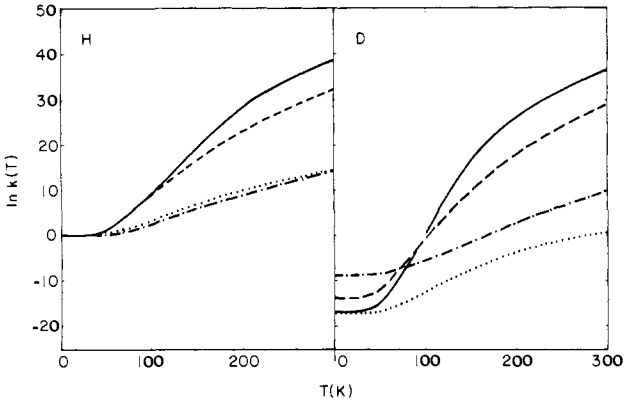

Figure 1. Illustration of the effects of anharmonicity in the potential corresponding to the low-frequency vibration. Dashed curves: harmonic potentials corresponding to CH-stretching vibrations and the low-frequency vibration; $\omega = 2960$ cm^{-1}, $\Omega = 200$ cm^{-1}, $\bar{R} - 2\xi = 1.5$ Å. Dotted curves: Morse potential for the low-frequency vibration; parameters as above, together with $X = 4$ cm^{-1}. Solid curves: U^+ as the potential for the low-frequency vibration; parameters as above, together with $K^2 = 7200$ cm^{-1}. Dot-dashed curves: U^- as the potential for the low-frequency vibration; parameters as above, together with $K^2 = 7200$ cm^{-1}.

because the energy levels are more closely spaced (negative anharmonicity).

We therefore consider potentials of the form

$$U^{\pm}(R) = \tfrac{1}{2}E + \tfrac{1}{2}M\Omega^2(R - \bar{R})^2 \pm \tfrac{1}{2}[E^2 + K^2M\Omega^2(R - \bar{R})^2]^{1/2} \quad (9)$$

generated from two harmonic potentials by the introduction of a linear coupling:

$$U_1(R) = \tfrac{1}{2}M\Omega^2(R - \bar{R})^2$$

$$U_2(R) = E + \tfrac{1}{2}M\Omega^2(R - \bar{R})^2$$

$$U_{12}(R) = \tfrac{1}{2}KM^{1/2}\Omega(R - \bar{R}) \quad (10)$$

Unlike the Morse potential, these potentials are even functions of $(R - \bar{R})$. Moreover, they permit not only a decrease of the vibrational energy level spacing with increasing quantum number, as for the Morse potential, but also an increase. The latter situation, corresponding to $U^-(R)$, might apply to a system in which steric effects become important for large bending amplitudes. A disadvantage of the potentials in (10) is that their anharmonicity is governed by two parameters, namely E and K. To circumvent this problem we set $E = {}^1/_2K^2$ arbitrarily; this choice offers the largest anharmonic distortion compatible with the condition that both $U^+(R)$ and $U^-(R)$ are potentials with a single minimum. Rate constants calculated with these potentials appear in Figure 1. The solid lines, corresponding to U^+, have slopes $\mathrm{d}(\ln k)/\mathrm{d}T$ greater than those of the dashed lines (harmonic) because it becomes progressively easier to population higher vibrational levels of the potential U^+ as the temperature increases. The rate constants $k_{\mathrm{BA},wWvV}$ are themselves somewhat smaller than those for the harmonic potential, which leads to slightly lower absolute rate constants for U^+. The dot-dashed curve in Figure 1 corresponds to $U^-(R)$, for which it is progressively more difficult to populate the next higher vibrational energy level, and for which the rate constants $k_{\mathrm{BA},wWvV}$ increase slowly with vibrational quantum number, as for the Morse potential and unlike the harmonic potential. Consequently, the slopes $\mathrm{d}(\ln k)/\mathrm{d}T$ are small, although the absolute rate constants are larger than those for the harmonic potential.

For the systems examined in section 4, we have found that the harmonic potential and $U^+(R)$ are most useful. For small amplitudes R, the latter resemble harmonic potentials subject to quartic anharmonicity as, e.g., for non-totally symmetric bending modes. We were unable to obtain slopes $\mathrm{d}(\ln k)/\mathrm{d}T$ as large as those observed experimentally with either the Morse potential or $U^-(R)$ and physically reasonable values for the adjustable parameters.

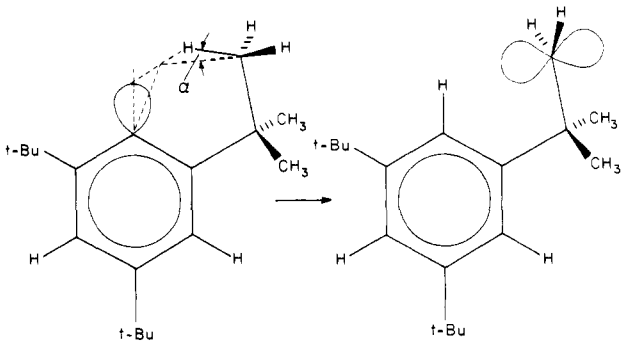

Figure 2. Schematic diagram of the isomerization of 2,4,6-tri-*tert*-butylphenyl to 3,5-di-*tert*-butylneophyl, showing the angle α, which is used to define ω(alkyl).

3. Choice of Parameter Values

The model described in section 1 gives a highly simplified description of the actual transfer process. Its success depends to a large extent on the ability of the model parameters to represent properties of the real system. During the transfer, the hydrogen atom moves along a path which in general does not correspond to a specific normal mode of the reactant. To represent this situation, we choose the parameter ω, which describes the hydrogen motion, and the parameters $\bar{R}$ and ξ, which describe the hydrogen path, according to the following rules: (i) $\bar{R} - 2\xi$ is equated with the shortest distance that the hydrogen must travel between its equilibrium positions in the initial and final states; (ii) for the XH bond (X = A or B), ω is written as

$$\omega = \omega_s \cos^2 \alpha + \omega_b \sin^2 \alpha \quad (11)$$

where ω_s and ω_b are the XH-stretching and -bending frequencies, respectively, and α is the angle between the XH bond and the line connecting X with the midpoint of the tunneling path (see Figure 2). If the structure of the reactants and products is known, this procedure is unambiguous. Isotopic substitution changes ω_s and ω_b but not the angles or the distances. Appropriate spectroscopic frequencies are used. Reduced masses μ are those appropriate to X–H(D) bonds. Bond lengths are standard.

The properties of the low-frequency oscillation are treated as adjustable parameters within a range of physically acceptable values. If the onset of the temperature dependence, i.e., the highest temperature for which $k(T) \approx k(0)$, is known, the frequency of Ω can be determined with good accuracy. However, it is not known for most of the reactions included in this paper. The search for the optimum value of Ω has been confined to the interval 0–200 cm^{-1}, the upper limit being suggested by the nature of the reactions. It is found that values in the upper part of this interval give the best agreement in most cases. The reduced mass M is similarly restricted to a number of values dictated by the nature of the oscillating groups. In the anharmonic version of the model, the parameter K is varied freely.

The exothermicity of the reaction is usually known or can be estimated from tabulated bond dissociation energies. To avoid strong oscillations in $k(T)$ with exothermicity due to accidental resonances with final-state levels, the width of these final levels is equated with one-half of their harmonic separation, i.e., $\hbar\Omega/2$. The resulting density of states ρ is a smooth function of the initial-state energy ϵ_{vV}.

4. Applications

A. Isomerization of Sterically Hindered Aryl Radicals. Rate constants for the isomerization of 2,4,6-tri-*tert*-butylphenyl to 3,5-di-*tert*-butylneophyl and the perdeuteriobutyl analogue have been measured by Brunton et al.[4] The reaction and its probable geometry are depicted schematically in Figure 2. From the large deuterium isotope effect in combination with the non-Arrhenius character of the temperature dependence of the rate constants,

(4) Brunton, G.; Gray, J. A.; Griller, D.; Barclay, L. R. C.; Ingold, K. U. *J. Am. Chem. Soc.* **1978**, *100*, 4197; private communication.

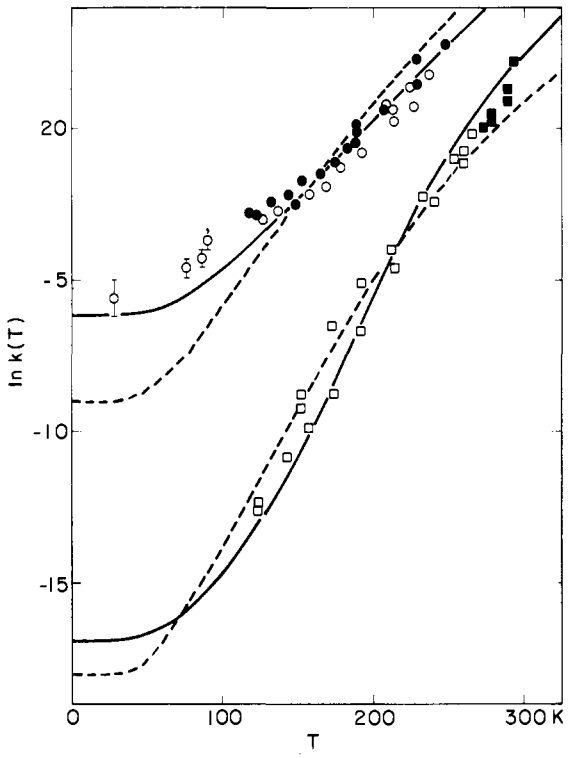

Figure 3. Plot of ln $k(T)$ against T for the isomerization of 2,4,6-tri-*tert*-butylphenyl (circles) and its perdeuteriobutyl analogue (squares) in solution (open) and in a solid matrix (solid). Circles with error bars refer to data considered less certain by the authors (ref 4). Dashed curves: harmonic potentials corresponding to CH-stretching vibrations and the low-frequency vibration. Solid curves: U^+ as the potential corresponding to the low-frequency vibration. Parameter values are given in the text.

the authors concluded that the reaction proceeds by tunneling. They interpreted their data in terms of a one-dimensional potential-energy barrier; however, the most successful of these barriers, namely the Eckart barrier, leads to parameter values which differ drastically from the equilibrium properties of CH bonds in the reactant and product. In our previous note,[5] we reinterpreted the data in terms of a two-dimensional harmonic model of the type described in part 1. Here we refine this application by lifting a number of artificial restrictions introduced in the interest of expediency.

The exothermicity of this isomerization is about 40 kJ/mol. We consider a transition state in which the CHC reaction plane coincides with the plane of the aromatic ring and neglect torsional motions. The tunneling distance $\bar{R} - 2\xi$ is estimated to be 1.34 Å, or $\bar{R}$ = 3.51 Å with 2ξ = 2.17 Å. From the rules given in section 3 we deduce that the effective high frequencies are ω^H(methyl) = 2811 cm^{-1}, ω^H(aryl) = 2794 cm^{-1}, ω^D(methyl) = 2023 cm^{-1}, and ω^D(aryl) = 2097 cm^{-1}. Apparently the low-frequency vibration involves bending of the methyl group, or the entire *tert*-butyl group, toward the radical center. We take the corresponding mass M to be the geometric mean of the reduced masses of the methyl and *tert*-butyl groups, or about 25 g/mol.

Experimental and calculated rate constants appear in Figure 3. When the potential for the low-frequency motion is harmonic and Ω = 150 cm^{-1}, J = 64 cm^{-1} for ζ = 1.625, and $\bar{R}$ = 3.4 Å, the dashed curve is obtained. The solid curve corresponds to the anharmonic version of the model with K^2 = 6120 cm^{-1}, Ω = 170 cm^{-1}, J = 60 cm^{-1}, and $\bar{R}$ = 3.3 Å. Although these equilibrium separations $\bar{R}$ are somewhat smaller than the value determined from molecular models, a 5° change in one bond angle is sufficient to eliminate the discrepancy. We conclude that the model gives a satisfactory account of the reaction, with the anharmonic version clearly superior to the harmonic version.

(5) Siebrand, W.; Wildman, T. A.; Zgierski, M. Z. *Chem. Phys. Lett.* **1983**, *98*, 108.

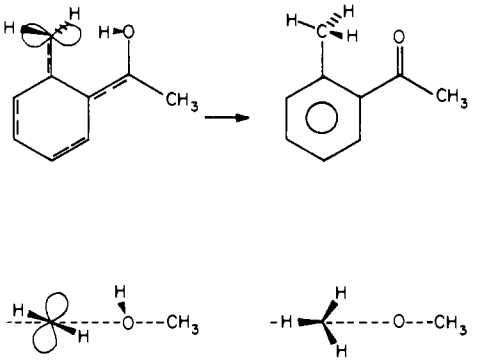

Figure 4. Reaction geometry proposed for the conversion of the cis enol to 2-methylacetophenone.

B. Enol–Ketone Transformation of 2-Methylacetophenone. Rate constants for conversion of the tautomeric cis enol to 2-methylacetophenone have been measured by Scaiano[6] and in great detail by Grellmann et al.[7] On the basis of the large deuterium isotope effect and the non-Arrhenius temperature dependence of the rate constants, the latter authors concluded that the reaction proceeds by tunneling. The kinetic scheme offered to interpret the observed rate constants involved a transition between two rotamers via a C–OH torsion, in qualitative agreement with our proposal that low-frequency modes play an essential role in the hydrogen transfer.

The reaction geometry is depicted in Figure 4. The trans enol cannot be the reactive conformer because the tunneling distance is too large (about 2.8 Å) and because the relative orientation of the OH bond being broken and the CH bond being formed is most unfavorable. On the other hand, steric interactions make the cis enol energetically unfavorable, although the tunneling distance is only about 1 Å. The reactant must adopt a conformation in which the hydroxyl group lies outside the ring plane, as in Figure 4. The methylene group may also twist somewhat to accommodate the incoming hydrogen. The exothermicity of this reaction has been estimated to be 160 kJ/mol on the basis of group increments.[8] We assume a larger value in our calculations, namely 200 kJ/mol, to include steric effects.

For the given enol conformation, we neglect torsions and set ω^H(hydroxyl) = 2503 cm^{-1}, ω^H(methyl) = 2271 cm^{-1}, ω^D(hydroxyl) = 1844 cm^{-1}, and ω^D(methyl) = 1625 cm^{-1}. Grellmann et al.[7] have estimated from molecular models that the shortest tunneling distance is 1.8 ± 0.2 Å, or $\bar{R}$ = 3.9 ± 0.2 Å. We set the reduced mass for the low-frequency mode equal to the reduced mass of the hydroxyl group, 15 g/mol. For hydrogen transfer between oxygen and carbon, ζ is 1.58 in eq 5.

If a harmonic potential is used for the low-frequency motion, we obtain the dashed curves in Figure 5 with Ω = 120 cm^{-1} and J = 491 cm^{-1}. Although the parameters which provide this "best" fit (for the harmonic version) are reasonable, the fit is not good for $T > 200$ K. There is some improvement in the calculated rate constants when anharmonicity is introduced. Because the exothermicity is large, anharmonicity of the high-frequency mode may also be important, particularly for the final state. After performing a number of calculations with anharmonicities of 8, 10, 12, 15, and 20 cm^{-1}, we chose to set the anharmonicity of the Morse potentials at 10 cm^{-1} for the OH and CH oscillators. The solid curve in Figure 5 is obtained when K^2 = 5040 cm^{-1} and J = 1.2 × 10^4 cm^{-1}, and the dotted curve corresponds to K^2 = 6860 cm^{-1} and J = 1.8 × 10^4 cm^{-1}. In both cases Ω = 140 cm^{-1} and $\bar{R}$ = 4.1 Å.

As in all of the examples treated in this paper, we have chosen to vary Ω by steps of 10 cm^{-1}, K^2 by steps equal to Ω, and $\bar{R}$ by steps of 0.1 Å; hence it may be possible to obtain a superior fit by further refinement of the parameter values. However, we

(6) Scaiano, J. C. *Chem. Phys. Lett.* **1980**, *73*, 319.
(7) Grellmann, K.-H.; Weller, H.; Tauer, E. *Chem. Phys. Lett.* **1983**, *95*, 195.
(8) Haag, R.; Wirz, J.; Wagner, P. J. *Helv. Chim. Acta* **1977**, *60*, 2595.

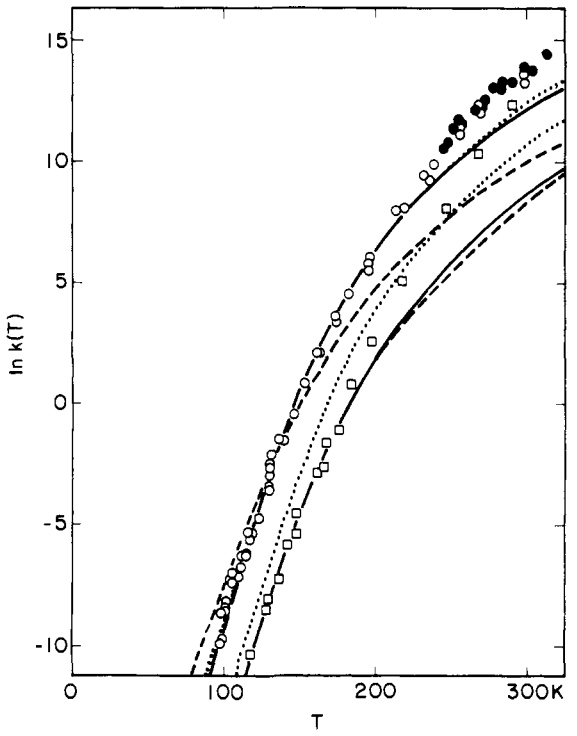

Figure 5. Plot of ln $k(T)$ against T for the conversion of the cis enol to 2-methylacetophenone (circles) and the deuterated analogue (squares). Solid circles are from ref 6, and all other data are from ref 7. Dashed curves: harmonic potentials corresponding to OH- and CH-stretching vibrations and the low-frequency vibration. Solid and dotted curves: Morse potentials corresponding to the bond-stretching vibrations and U^+ as the potential for the low-frequency vibration. Parameter values are given in the text.

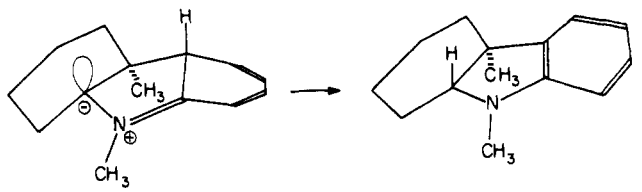

Figure 6. Formation of a hexahydrocarbazole by a 1,4-sigmatropic hydrogen shift.

believe that the success of the model in its present form is limited by its inability to describe the complicated internal motions of the reactant at $T > 200$ K; bending is included in an artificial way, and torsions, which profoundly affect the reaction geometry, are completely neglected. We conclude that a more sophisticated version, incorporating three or more modes, is required.

C. Sigmatropic Hydrogen Shift in a Hexahydrocarbazole. Rate constants for the isomerization depicted in Figure 6, and for its deuterated analogue, have been measured by Grellmann et al.[9] These authors interpreted the large deuterium isotope effect and the non-Arrhenius temperature dependence of the rate constant as due to hydrogen tunneling. From our molecular models, the tunneling distance is estimated to be 3.1 ± 0.1 Å, or $\bar{R} = 5.3$ Å. The exothermicity of this isomerization is unknown. Grellmann et al. achieved a good fit to the observed rate constants with a symmetrical Eckart barrier; for purposes of comparison we assume that the exothermicity is zero.

Plainly, the relative orientation of the CH bond being broken and the CH bond being formed is not very favorable to the reaction. Bending modes must play a major role in the transfer, but bond bending alone does not lead to bond cleavage: hence for a proper description of the reaction both CH bending and CH stretching should be included, together with their coupling. This would require generalization of the model. The carbon skeleton is highly strained, but inspection of models suggests that the low-frequency twisting mode in which the terminal rings rotate in opposite directions will have a strong effect on the relative orientation of the CH bond to be broken and that to be formed.

(9) Grellmann, K.-H.; Schmitt, U.; Weller, H. *Chem. Phys. Lett.* **1982**, *88*, 40.

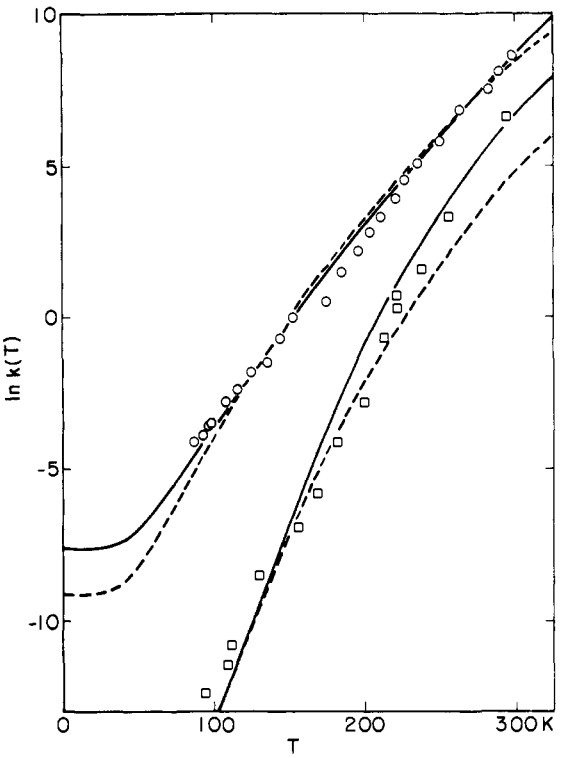

Figure 7. Plot of ln $k(T)$ against T for the reaction depicted in Figure 6 (circles) and the deuterated analogue (squares). Dashed curves: harmonic potentials corresponding to CH-stretching vibrations and the low-frequency vibration. Solid curves: U^+ as the potential corresponding to the low-frequency vibration. Parameter values are given in the text.

Accepting the limitations of our model, we use bending-mode frequencies for the high-frequency modes: ω^H(initial) = 1588 cm^{-1}, ω^H(final) = 1712 cm^{-1}, ω^D(initial) = 1288 cm^{-1}, and ω^D(final) = 1361 cm^{-1}. A value cannot readily be assigned to the reduced mass of the low-frequency oscillator; we investigated the values 15, 30, and 45 g/mol, which cover the range of probable values.

Calculated rate constant curves in Figure 7 were obtained for $\Omega = 140$ cm^{-1}, $M = 15$ g/mol, $\zeta = 1.625$, $\bar{J} = 11$ cm^{-1}, and $\bar{R} = 3.6$ Å with the harmonic version (dashed curves), or $\bar{J} = 8$ cm^{-1} and $K^2 = 8960$ cm^{-1} with the anharmonic version (solid curves). It was not possible to reproduce satisfactorily the observed rate constants with $\bar{R} = 5.3$ Å, which is not surprising, since the expression $\bar{R} - 2\xi$ has no physical meaning in the present case where the $\bar{R}$ and ξ distances are nearly at right angles. Hence we do not believe that the discrepancy contradicts the assumption that the reaction proceeds by a 1,4-sigmatropic hydrogen shift. Clearly the problem lies in the treatment of the bending modes. The version of the model described in section 1 applies to collinear bond stretching. Effects of bond bending are included in an artificial way by taking a linear combination of stretching and bending frequencies, as described in section 3. However, the overlap integrals S_{wp} defined by eq 4 cannot describe displaced oscillators for bending vibrations. When bending is important, bending and stretching modes must be included separately in a more sophisticated version of the model.

D. Hydrogen Abstraction by Free Radicals in Crystalline Dimethylglyoxime. If dimethylglyoxime crystals at low temperature are exposed to ionizing radiation, radical pairs are formed. A pair at opposite corners of a face of a unit cell may convert into a pair at adjacent corners by hydrogen abstraction. As in the preceding examples, deuterium isotope and temperature effects provide evidence for tunneling. Rate constants have been reported by Yakimchenko and Lebedev[10] and by Toriyama et al.[11] The

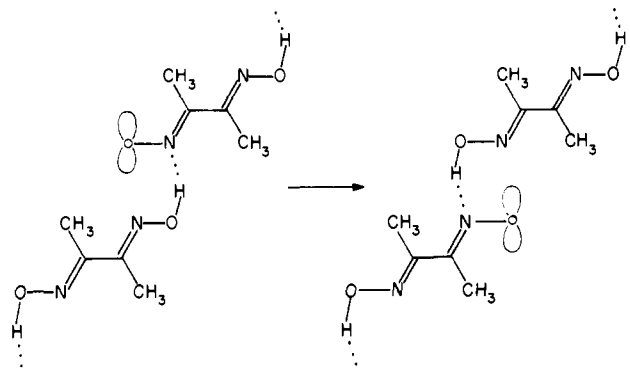

Figure 8. Relative orientation of a dimethylglyoxime radical and a neighboring molecule in the crystal.

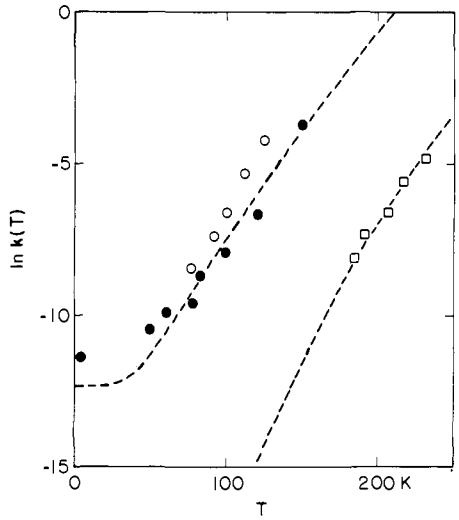

Figure 9. Plot of ln $k(T)$ against T for radical-pair conversion in dimethylglyoxime (circles) and in the deuterated analogue (squares). Solid circles are from ref 11, and all other data are from ref 10. Dashed curves correspond to harmonic potentials for OH-stretching vibrations and the low-frequency vibration. Parameter values are given in the text.

latter authors have fitted the observations to an Eckart potential.

The reaction is depicted in Figure 8. We take the exothermicity to be zero. From the crystal structure of dimethylglyoxime,[12] the tunneling distance is estimated to be 2.3 Å, or $\bar{R}$ = 4.2 Å. We are unable to reproduce the observed rate constants with such large values for $\bar{R}$, regardless of whether we treat the low-frequency mode as harmonic or anharmonic. In fact, the relative orientation of the radical and the neighboring molecule in the irradiated crystal is not known. It is possible that the radical is oriented more favorably than the parent molecule; perhaps it forms a stronger hydrogen bond with the neighboring molecule. With this justification, we take OHO collinear. The corresponding value $\bar{R}$ is 3.2 Å. We set ω^H = 3407 cm^{-1} and ω^D = 2150 cm^{-1}. The reduced mass of the low-frequency oscillator is that appropriate to a pair of dimethylglyoxime molecules, namely 58 g/mol. For transfer between oxygen atoms, ζ is 2.275.

The dashed curve in Figure 9 corresponds to Ω = 120 cm^{-1}, $\bar{J}$ = 10 cm^{-1}, and $\bar{R}$ = 2.9 Å with the harmonic version of the model. This value of $\bar{R}$ is somewhat smaller than expected, but the discrepancy is not serious. If there is a strong hydrogen bond between the radical and the neighbor, $\bar{J}$ is expected to be large, but these values are extremely sensitive to the values of other parameters (see section 5). The agreement between the available data and the calculated rate constants is not improved by introducing anharmonicity in the low-frequency mode.

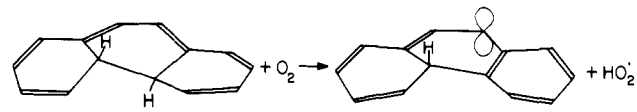

Figure 10. Reaction of *trans*-4a,4b-dihydrophenanthrene with molecular oxygen.

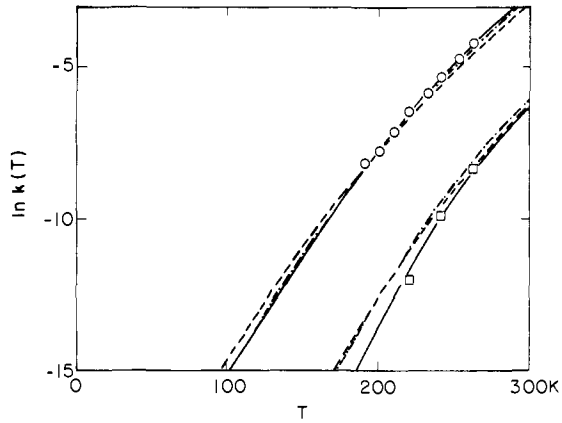

Figure 11. Plot of ln $k(T)$ against T for the initiation step in the thermal reaction of 4a,4b-dihydrophenanthrene with molecular oxygen in solution. Dashed and dot-dashed curves: harmonic potentials for CH- and OH-stretching vibrations and for the low-frequency vibration. Solid curves: U^+ as the potential corresponding to the low-frequency vibration. Parameter values are given in the text.

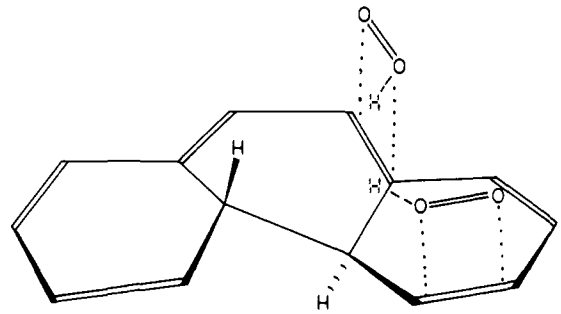

Figure 12. Possible orientations of oxygen in the reactive complex with *trans*-4a,4b-dihydrophenanthrene.

E. Hydrogen Transfer from Dihydrophenanthrene to Oxygen in Solution. According to Bromberg et al.[13] the self-initiation step in the thermal reaction of 4a,4b-dihydrophenanthrene with molecular oxygen in solution is the abstraction of a hydrogen atom by oxygen, as depicted in Figure 10. These authors propose that the exothermicity of this step is essentially zero and that the reaction takes place in a specific configuration of the reactants. Although such complexes between an aromatic hydrocarbon and oxygen are known,[14] no information is available on the structure of the reactive complex. The present model offers the possibility of gaining such information by analysis of rate constants.

To represent the case in which the CH bond being broken is collinear with the OH bond being formed, we put ω^H(alkyl) = 2914 cm^{-1}, ω^H(hydroxyl) = 3407 cm^{-1}, ω^D(alkyl) = 2095 cm^{-1}, and ω^D(hydroxyl) = 2510 cm^{-1}. For the low-frequency oscillator we take the reduced mass of the dihydrophenanthrene–oxygen pair to be 27 g/mol. With Ω = 160 cm^{-1}, $\bar{J}$ = 0.52 cm^{-1}, ζ = 1.58 and $\bar{R}$ = 3.1 Å, we obtain the dashed curve in Figure 11 for the harmonic version of the model. If α in eq 11 is assumed to be 30°, then ω^H(alkyl) = 2529 cm^{-1}, ω^H(hydroxyl) = 2914 cm^{-1}, ω^D(alkyl) = 1861 cm^{-1}, and ω^D(hydroxyl) = 2135 cm^{-1}, which

(10) Yakimchenko, O. Ye.; Lebedev, Ya. S. *Int. J. Radiat. Phys. Chem.* **1971**, *3*, 17. The data also appear in: Goldanskii, V. I. *Annu. Rev. Phys. Chem.* **1976**, *27*, 85.

(11) Toriyama, K.; Nunome, K.; Iwasaki, M. *J. Am. Chem. Soc.* **1977**, *99*, 5823.

(12) Merritt, L. L., Jr.; Lanterman, E. *Acta Crystallogr.* **1952**, *5*, 811.

(13) Bromberg, A.; Muszkat, K. A.; Fischer, E. *Chem. Commun.* **1968**, 1352. Bromberg, A.; Muszkat, K. A.; Fischer, E.; Klein, F. S. *J. Chem. Soc., Perkin Trans. 2* **1972**, 588.

(14) McGlynn, S. P.; Azumi, T.; Kinoshita, M. "Molecular Spectroscopy of the Triplet State"; Prentice-Hall: Englewood Cliffs, NJ, 1969; p 285ff.

leads to the dot-dashed curve in Figure 11 for Ω = 140 cm^{-1}, $\bar{J}$ = 0.32 cm^{-1}, and $\bar{R}$ = 3.2 Å. The available data do not warrant a choice between these sets of a parameter values. With the anharmonic low-frequency potential, the solid curve in Figure 11 is obtained when Ω = 160 cm^{-1}, $\bar{J}$ = 4.9 cm^{-1}, $\bar{R}$ = 3.1 Å, K^2 = 10240 cm^{-1}, and the arrangement is collinear. If the reactive complex results from overlap of π-orbitals of the hydrocarbon and oxygen, as in the hypothetical structures in Figure 12, and if the oxygen molecule lies 2–3 Å above the π-plane, then the expected tunneling distance is near the 1.1 Å suggested by our model calculations. We conclude that the present model can reproduce the available experimental data and may provide some new information on the structure of the reactive complex. The observed rate constants cover a rather narrow temperature range, however, and further experimental work, on deuterium transfer in particular, is necessary before more detailed structural information can be obtained.

F. Other Examples. Two other hydrogen-transfer reactions have been studied over a wide range of temperature: the decay of methyl radicals in certain solid matrices[15] and the tautomerization of *meso*-tetraphenylporphine.[16] Methyl radicals in a methanol or ethanol matrix will abstract hydrogen atoms from host molecules. A simple version of our model, which included only resonance interactions, successfully reproduced the temperature dependence of the "first-order" rate constant for decay of methyl radicals in an ethanol matrix, as reported earlier.[5] However, the decay is non-exponential, presumably because the radicals occupy a distribution of sites, each characterized by a different rate constant.[17] The time dependence of the decay is then related to the Laplace transform of the initial distribution of rate constants, which can be characterized by a "most probable" rate constant. Because further experimental work is needed to determine the temperature dependence of the most probable rate constant, the analysis of this system is postponed until a later publication.

The kinetics of the intramolecular hydrogen migration between nitrogen atoms of *meso*-tetraphenylporphine (TPP) have been studied over a wide range of temperature for both isotopes.[16] In this case the carbon–nitrogen skeleton is quite rigid and inflexible. Therefore, the effect of low-frequency motions on the oscillations of the NHN barrier is expected to be very small, and the temperature dependence is governed by the high-frequency hydrogenic modes. The geometry of the molecule indicates that NH-bending modes play an essential role. The structure of TPP in the tetragonal crystal[18] places a "half hydrogen" at each nitrogen, but in the triclinic crystal[19] the hydrogens are located at opposite nitrogens with a H···H separation equal to the sum of the van der Waals radii. The symmetry of this tautomer is consistent with the observation of three NH vibrations in the infrared spectrum;[20] five infrared-active vibrations are expected if the hydrogens are located at adjacent nitrogens. Presumably, the hydrogens move in concert to retain this relative orientation. The effects of isotopic substitution on the infrared spectrum suggest that the two NH oscillators are coupled and that there is little coupling between the N and H atom motions.[21] Coupling of the NH-bending and NH-stretching vibrations has not been studied, although it is certain to occur given the environment. A model similar to the one described here, but which includes coupled NH bending and NH stretching and which excludes the low-frequency N···N motion, predicts the onset of the temperature dependence of the rate constant for hydrogen tranfer below 200 K. The observed rate constant remains nearly linear in T to 200 K, which is the low-temperature limit of the available data.[22] Because no information is available on the form of the NH vibrational potential, other than the fundamental frequencies, and because the calculated results are sensitive to the magnitude of the anharmonicities of and the couplings between the NH-stretching and NH-bending modes, the temperature and isotope effects on the rate constants have not yet been reproduced satisfactorily.

5. Discussion

The examples discussed in the preceding section comprise the best hydrogen tunneling data presently available. They permit a reasonably comprehensive comparison of our approach with the conventional tunneling treatment, discussed at length in Bell's book.[18] Conventionally, one tries to explain the observed temperature dependence of hydrogen and deuterium transfer rate constants in terms of a one-dimensional potential-energy barrier to be crossed by the mobile atom. This is essentially an empirical approach, subject to the consistency requirement that the barrier should be isotope independent. Among the analytical barrier shapes tried in this fashion, the Eckart barrier is perhaps the most successful. Typically, these barriers are very low, amounting to 1–2 quanta of the XH-stretch mode involved in the transfer: this is required to account for the strong temperature dependence of the transfer at low temperatures.

Since these barriers differ greatly from the barriers that can be constructed from the spectroscopically known equilibrium properties of reactants and products, they have no firm theoretical basis. One may speculate that they represent the non-equilibrium situation most favorable for transfer, but no method is available to construct them from spectroscopically or quantum-chemically known potentials. To analyze transfer data, it seems preferable to focus on quantities that, at least in principle, can be calculated theoretically or derived unambiguously from other observables.

In our model, the observed temperature dependence of the transfer is not ascribed to static properties of the barrier such as its shape or height but ascribed to dynamic properties, namely thermal motion due to vibrations of the atoms between which the hydrogen is transferred. If these vibrations are included, we can account satisfactorily for the observed temperature dependence without invoking unphysically low barriers. The calculations presented in the preceding section lead to frequencies in the range 120–170 cm^{-1} for these vibrations, which we attribute to bending motions involving the carbon, nitrogen, and oxygen atoms carrying the hydrogen. This assignment is supported by the observation that the vibrations are anharmonic but do not resemble Morse oscillators, the leading anharmonic term in the potential being quartic rather than cubic. In two of the examples discussed this picture requires revision. In the example of section 4B, the temperature dependence is not satisfactorily reproduced at high temperatures. However, on the basis of molecular models, we conclude that more than one low-frequency mode must be active here, namely a twisting mode as well as a bending mode. Hence the model needs to be generalized for this molecule. In the example of hydrogen transfer inside a free-base porphyrin, discussed in section 4, the available low-frequency motions of the porphyrin ring system are ineffective in changing the separation of the nitrogen atoms carrying the hydrogen. Hence, to account for transfer in this system, two high-frequency hydrogenic modes are required. The quantitative inaccuracy of the model in these two cases can thus be related directly to simplifying assumptions made for reasons of expediency.

In all cases considered, both the absolute magnitude of the rate constant and the ratio of hydrogen and deuterium rate constants are very sensitive to the equilibrium tunneling distance $\bar{R} - 2\xi$,

(15) Le Roy, R. J.; Murai, H.; Williams, F. *J. Am. Chem. Soc.* **1980**, *102*, 2325.

(16) Hennig, J.; Limbach, H.-H. *J. Chem. Soc., Faraday Trans. 2* **1979**, *75*, 752. Limbach, H.-H.; Hennig, J. *J. Chem. Phys.* **1979**, *71*, 3120. Stilbs, P.; Moseley, M. E. *J. Chem. Soc., Faraday Trans. 2* **1980**, *76*, 729. Limbach, H.-H.; Hennig, J.; Gerritzen, D.; Rumpel, H. *Faraday Discuss. Chem. Soc.* **1982**, *74*, 229.

(17) (a) Doba, T.; Ingold, K. U.; Siebrand, W. *Chem. Phys. Lett.* **1984**, *103*, 339. (b) Doba, T.; Ingold, K. U.; Siebrand, W.; Wildman, T. A. *J. Phys. Chem.*, in press.

(18) Hamor, M. J.; Hamor, T. A.; Hoard, J. L. *J. Am. Chem. Soc.* **1964**, *86*, 1938.

(19) Silvers, S. J.; Tulinsky, A. *J. Am. Chem. Soc.* **1967**, *89*, 3331.

(20) Tulinsky A. *Ann. N. Y. Acad. Sci.* **1973**, *206*, 47.

(21) Mason, S. F. *J. Chem. Soc.* **1958**, 976. Alben, J. O.; Choi, S. S.; Adler, A. D.; Caughey, W. S. *Ann. N. Y. Acad. Sci.* **1973**, *206*, 278.

(22) Limbach, H.-H.; Hennig, J.; Stulz, J. *J. Chem. Phys.* **1983**, *78*, 5432.

(23) Bell, R. P. "The Tunnel Effect in Chemistry"; Chapman and Hall: London, 1980.

which is known only approximately. Since an error of 0.1 Å in $\bar{R} - 2\xi$ may cause an error in $k(T)$ approaching a factor of 10^4, it is not feasible to calculate absolute rate constants. By the same token, it is not possible to fix $\bar{J}$ accurately in our present calculations where $k(T)$ is used as an input parameter: the values of $\bar{J}$ used in the examples thus show wide variations. Nevertheless, these $\bar{J}$ values may still provide a useful indication of the absolute accuracy of $\bar{R} - 2\xi$. On physical grounds one expects $\bar{J}$ to increase sharply (rough exponentially) with decreasing $\bar{R} - 2\xi$. However, in our applications, small distances often lead to small couplings. This probably means that $\bar{R} - 2\xi$ has been underestimated in these cases and that the resulting error is compensated by a low value of $\bar{J}$.

These considerations suggest a specific approach to improve the model. The coupling $\bar{J}$ can in principle be removed as an adjustable parameter, since $J_{AB}(R)$ is amenable to quantum-chemical calculation. In several of the examples presented, this would undoubtedly give rise to a substantial change of the other parameters and probably a poorer reproduction of the experimental data. This in turn would indicate the need for a more accurate description of the reaction path, specifically for the inclusion of an XH-bending along with an XH-stretching coordinate. Such improvements will be considered in forthcoming publications.

The examples treated here show, however, that the model in its simple form is adequate for a semiquantitative interpretation of hydrogen-tunneling reactions, especially in systems approaching collinearity. It gives a much more realistic picture of the transfer than the conventional tunneling approach and may permit one to draw specific conclusions about the mechanism of the transfer. Its assignment of numbers to specific molecular properties suggests new experiments and new calculations, which, we hope, will stimulate research in this area.

Acknowledgment. We are grateful to Keith Ingold for his comments and encouragement.

Registry No. 2,4,6-Tri-*tert*-butylphenyl, 53054-78-7; 2-methylacetophenone *cis*-enol, 85562-08-9; *trans*-2,3,4,4a,9,9a-hexahydro-4a,9-dimethylindole, 20890-47-5; dimethylglyoxime, 95-45-4; *trans*-4a,4b-dihydrophenanthrene, 33431-13-9; methyl, 2229-07-4; *meso*-tetraphenylporphine, 917-23-7.

Monte Carlo Studies of a Dilute Aqueous Solution of Benzene

P. Linse,*† G. Karlström,† and B. Jönsson‡

Contribution from Physical Chemistry 1 and 2, Chemical Center, University of Lund, S-220 07 Lund, Sweden. *Received September 21, 1983*

Abstract: A dilute aqueous solution of benzene has been examined by Monte Carlo simulations using pairwise additive potentials obtained from ab initio quantum chemical calculations. The water molecules in the first hydration shell around a benzene molecule show a preferential orientation according to the electrostatic dipole–quadrupole interaction. However, the water–water distribution functions for molecules close to the benzene molecule show only small deviations from what is found in pure water. The two models studied, periodic, boundary conditions and the cluster model, have a stronger influence on the properties calculated than the presence of a benzene molecule.

Dilute aqueous solutions are of fundamental importance, and in recent years, computer simulation methods such as Monte Carlo (MC) and molecular dynamic (MD) techniques have provided detailed molecular information on the structure of water around a solute molecule. Such structural and dynamic information is usually very difficult to extract from experiments on dilute solutions. Most computer simulations of aqueous solutions have so far been concerned with small, often spherical, solutes. The solute–water interaction has been described by both empirical[1-4] and quantum mechanical potentials.[5-10] Examples of hydrophobic solutes investigated are methane[5,6] and argon,[7] but polar nonionic solutes such as methanol,[8] ethanol,[9] and formaldehyde[10] have also been considered. In some cases, the solvation effects on the intramolecular structure have been studied explicity—examples are methanol,[8] butane,[11] and hydrogen peroxide.[12] Computer simulations have also been performed on electrolyte solutions[13-18] and on solvation of fragments of biomolecules.[19,20]

A common goal of these simulations has been to study how the solute molecule influences the solvent structure. The generally accepted picture of hydrophobic hydration, arising both from experiment and computer simulations, is that the loose network of hydrogen bonds is strengthened around the nonpolar solute, giving a more ordered water structure.[21,22] On the other hand, the interaction between an ion and water is quite different. The prevalent picture of ions in aqueous solutions stems from the work of Gurney[23] and Frank and Wen.[24] In this case, the orientation of water molecules close to the ion is governed by the ion–water interaction, and the network of hydrogen bonds is partially destroyed.

†Physical Chemistry 1.
‡Physical Chemistry 2.

(1) Geiger, A.; Rahman, A.; Stillinger, F. H. *J. Chem. Phys.* **1979**, *70*, 263.
(2) Okazaki, S.; Nakanishi, K.; Touhara, H.; Adachi, Y. *J. Chem. Phys.* **1979**, *71*, 2421.
(3) Okazaki, S.; Nakanishi, K.; Touhara, H.; Watanabe, N.; Adachi, Y. *J. Chem. Phys.* **1981**, *74*, 5863.
(4) Pangali, C.; Rao, M.; Berne, B. J. *J Chem. Phys.* **1979**, *71*, 2975, 2982.
(5) Swaminathan, S.; Harrison, S. W.; Beveridge, D. L. *J. Am. Chem. Soc.* **1978**, *100*, 5705.
(6) Owicki, J. C.; Scheraga, H. A. *J Am. Chem. Soc.* **1977**, *99*, 7413.
(7) Alagona, G.; Tani, A. *J. Chem. Phys.* **1980**, *72*, 580.
(8) Bolis, G.; Corongiu, G.; Clementi, E. *Chem. Phys. Lett.* **1982**, *86*, 299.
(9) Alagona, G.; Tani, A. *Chem. Phys. Lett.* **1982**, *87*, 337.
(10) Mehrotra, P. K.; Beveridge, D. L. *J. Phys. Chem.* **1980**, *102*, 4287.
(11) Jorgensen, W. L. *J. Chem. Phys.* **1982**, *77*, 5757.
(12) Jönsson, B.; Romano, S.; Karlström, G. *Int. J. Quantum Chem.* **1984**, *25*, 503.
(13) Briant, C. L.; Burton, J. J. *J. Chem. Phys.* **1976**, *64*, 2888.
(14) Rao, M.; Berne, B. J. *J. Chem. Phys.* **1981**, *85*, 1498.
(15) Geiger, A. *Ber. Bunsenges. Phys. Chem.* **1981**, *85*, 52.
(16) Mazei, M.; Beveridge, D. L. *J. Chem. Phys.* **1981**, *74*, 6902.
(17) Engström, S.; Jönsson, B.; Jönsson, B. *J. Magn. Reson.* **1982**, *50*, 1.
(18) Lee, W. K.; Prohofsky, E. W. *J. Chem. Phys.* **1981**, *75*, 3040.
(19) Clementi, E.; Corongiu, G. *Biopolymers* **1981**, *20*, 551.
(20) Karplus, M.; McCammon, J. A. *CRC Crit. Rev. Biochem.* **1981**, *9*, 293.
(21) Franks, F. In "Water–A Comprehensive Treatise"; Franks, F. Ed.; Plenum Press: New York, 1972; Vol 2.
(22) Ben-Naim, A. "Water and Aqueous Solutions"; Plenum Press: New York, 1974.
(23) Gurney, R. W. "Ionic Processes in Solutions"; McGray-Hill: New York, 1953.
(24) Frank, H. S.; Wen, W. Y. *Discuss. Faraday Soc.* **1957**, *24*, 133.

0002-7863/84/1506-4096$01.50/0